Journal of the American College of Cardiology
© 2014 by the American College of Cardiology Foundation
Published by Elsevier Inc.

Vol. 63, No. 11, 2014
ISSN 0735-1097/$36.00
http://dx.doi.org/10.1016/j.jacc.2013.10.084

Cardiac Imaging

Diffuse Myocardial Fibrosis Evaluated by Post-Contrast T_1 Mapping Correlates With Left Ventricular Stiffness

Andris H. Ellims, MBBS,*† James A. Shaw, MBBS, PhD,*† Dion Stub, MBBS, PhD,*† Leah M. Iles, MBChB,*† James L. Hare, MBBS, PhD,*† Glenn S. Slavin, PhD,‡ David M. Kaye, MBBS, PhD,*† Andrew J. Taylor, MBBS, PhD*†

Melbourne, Victoria, Australia; and Bethesda, Maryland

Objectives The purpose of this study was to use cardiac magnetic resonance (CMR) imaging and invasive left ventricular (LV) pressure-volume (PV) measurements to explore the relationship between diffuse myocardial fibrosis and indexes of diastolic performance in a cohort of cardiac transplant recipients.

Background The precise mechanism of LV diastolic dysfunction in the presence of myocardial fibrosis has not previously been established.

Methods We performed CMR with T_1 mapping and obtained invasive LV PV measurements via a conductance catheter in 20 cardiac transplant recipients at the time of clinically-indicated coronary angiography.

Results Both post-contrast myocardial T_1 time and extracellular volume fraction correlated with β, the load-independent passive LV stiffness constant ($r = -0.71$, $p = 0.001$, and $r = 0.58$, $p = 0.04$, respectively). After multivariate analysis, post-contrast myocardial T_1 time remained the only independent predictor of β. No significant associations were observed between myocardial T_1 time and τ, the active LV relaxation constant, or other load-dependent parameters of diastolic function.

Conclusions Diffuse myocardial fibrosis, assessed by post-contrast myocardial T_1 time, correlates with invasively-demonstrated LV stiffness in cardiac transplant recipients. In patients with increased diffuse myocardial fibrosis, abnormal passive ventricular stiffness is therefore likely to be a major contributor to diastolic dysfunction. (J Am Coll Cardiol 2014; 63:1112–8) © 2014 by the American College of Cardiology Foundation

Myocardial fibrosis is a fundamental event in the development of cardiac failure (1), regardless of its etiology (2,3). In animal models, myocardial fibrosis is associated with worsening ventricular systolic function, abnormal cardiac remodeling, and increased ventricular stiffness (4). Myocardial fibrosis may be regional, as found in myocardial infarction due to coronary atherosclerosis, or diffuse, as observed in all forms of advanced cardiomyopathy. Diffuse myocardial fibrosis may be relevant in the pathogenesis of heart failure with a normal left ventricular (LV) ejection fraction, which accounts for as many as 50% of all cases of heart failure and carries a morbidity/mortality profile comparable to that of systolic heart failure (5). Although the detrimental effects of increasing myocardial fibrosis in heart failure still require further elucidation, a likely mechanism is diastolic dysfunction due to increased ventricular stiffness, which carries a poor prognosis in patients with cardiomyopathy in whom restrictive physiology develops (6).

See page 1119

Critical to our understanding of diffuse myocardial fibrosis and ventricular stiffness is the demonstration of a mechanistic link between these 2 observed phenomena. Using a histologically-validated cardiac magnetic resonance (CMR) imaging post-contrast T_1 mapping technique (7,8), we previously observed in patients with advanced heart

From the *Heart Centre, Alfred Hospital, Melbourne, Victoria, Australia; †Baker IDI Heart and Diabetes Research Institute, Melbourne, Victoria, Australia; and ‡GE Healthcare, Bethesda, Maryland. Dr. Ellims is supported by a combined Heart Foundation of Australia and National Heart and Medical Research Council Postgraduate Research Scholarship. Dr. Stub is supported by a Heart Foundation of Australia Scholarship and a Baker IDI Heart and Diabetes Institute Award. Dr. Iles is supported by a National Health and Medical Research Council Postgraduate Research Scholarship. Dr. Hare is supported by a Cardiac Society of Australia and New Zealand Research Investigatorship; and has a nonfinancial research agreement with GE Medical. Prof. Kaye is supported by a National Health and Medical Research Council program grant. Associate Professor Taylor is supported by a National Health and Medical Research Council project grant. Drs. Shaw and Slavin have reported that they have no relationships relevant to the contents of this paper to disclose.

Manuscript received July 24, 2013; revised manuscript received October 17, 2013, accepted October 28, 2013.

failure that increasing amounts of diffuse myocardial fibrosis, as suggested by shortened post-contrast myocardial T_1 time, are accompanied by worsening diastolic function. Subsequent studies using a similar T_1 mapping technique have observed correlations between post-contrast myocardial T_1 time and noninvasive estimates of LV diastolic function in other disease states, including diabetes mellitus (9,10) and hypertrophic cardiomyopathy (11). Alternative T_1 mapping approaches, including noncontrast (native) and extracellular volume (ECV) fraction techniques, have also been used to characterize myocardial tissue in other conditions such as cardiac amyloidosis (12), aortic stenosis (13), and systemic lupus erythematosus (14).

Although echocardiographic index of diastolic function have been validated against invasive LV pressure measurement (15,16), these methods are sensitive to the effects of loading conditions. Furthermore, it is virtually impossible to noninvasively ascertain the relative contributions of active ventricular relaxation, passive ventricular stiffness, volume loading, and other extrinsic factors to diastolic dysfunction. However, with the aid of accurate invasive pressure-volume (PV) measurement, LV diastole can be broken up into 2 basic components: a decaying curve relating to active ventricular relaxation and a passive filling pressure curve that increases monotonically with pressure. Tau (τ), the time constant of active LV relaxation, is prolonged in diastolic dysfunction, particularly in the presence of coexistent systolic dysfunction (17). Higher values of the passive LV stiffness constant (β) have been demonstrated in the presence of reduced ventricular compliance, consistent with intrinsic stiffening of the myocardium (18). In human subjects with diastolic dysfunction, derangements of both active relaxation and intrinsic stiffening have been implicated (19).

An investigation of the relationship between diffuse myocardial fibrosis and ventricular stiffness as a putative mechanism of diastolic dysfunction has not previously been described. We performed CMR with post-contrast T_1 mapping and obtained invasive LV PV measurements in a cohort of cardiac transplant recipients at the time of clinically-indicated coronary angiography to relate change in myocardial tissue composition to intrinsic mechanical properties of the myocardium during diastole.

Methods

Patient selection. All research was performed at the Alfred Hospital, Melbourne, Victoria, Australia. Twenty-seven consecutive cardiac transplant recipients referred for surveillance invasive coronary angiography were invited to participate. Exclusion criteria included chronic atrial fibrillation, histological evidence of allograft rejection, contraindications to CMR including pacemaker and defibrillator implantation, and significant renal dysfunction (estimated glomerular filtration rate [eGFR] <30 ml/min/1.73 m^2). Informed consent was obtained from all participants, and the study was conducted in accordance with the Alfred Hospital Ethics Committee's guidelines.

Abbreviations and Acronyms

CC = conductance catheter
CMR = cardiac magnetic resonance
ECV = extracellular volume
eGFR = estimated glomerular filtration rate
LGE = late gadolinium enhancement
LV = left ventricular
LVEDP = left ventricular end-diastolic pressure
PCWP = pulmonary capillary wedge pressure
PV = pressure-volume
TI = inversion time

Cardiac catheterization protocol. To measure right atrial pressure, right ventricular pressure, pulmonary artery pressure, and pulmonary capillary wedge pressure (PCWP), an introducer sheath was placed in the right femoral vein while the patients were under local anesthesia, and, under fluoroscopy, a 7-F balloon-tipped thermodilution catheter (7-F Arrow, Edwards Corp., Irvine, California) was introduced. The wedge position was confirmed fluoroscopically and by the profile of the accompanying pressure waveform, and the mean PCWP was recorded at end-expiration. Cardiac output was measured using the thermodilution technique. Standard invasive coronary angiography was then performed via right femoral artery access.

A conductance catheter (CC) was used to record simultaneous LV PV measurements (20,21). A 7-F CC (CD Leycom, Zoetermeer, the Netherlands) was advanced via right femoral artery access into the left ventricle under fluoroscopic guidance immediately after coronary angiography and connected to a PV signal processor (Inca, CD Leycom). Real-time continuous LV pressure and volume signals were recorded for at least 30 s with patients in the supine position. Volume calibration was performed using LV volumetric data obtained from the same-day CMR, and CC data analysis was performed with dedicated software (Conduct NT, CD Leycom). Load-dependent LV diastolic function was assessed by left ventricular end-diastolic pressure (LVEDP), and τ was calculated using a formula previously described by Weiss et al. (17). Load-independent LV diastolic function was evaluated by β, using an exponential equation representing the relationship of ventricular volume to pressure during passive filling (22): $P = P_B + Ae^{\beta V}$, where P is LV diastolic pressure, P_B is the pressure asymptote, A and β are fitting constants, and V is LV diastolic volume. Curve fitting to derive P_B, A, and β was performed using a graphing software package (Origin 8.5, OriginLab Corporation, Northampton, Massachusetts).

CMR protocol. We performed CMR on all patients using a clinical 1.5-T scanner (Signa HD 1.5-T, GE Healthcare, Waukesha, Wisconsin) on the same day that cardiac catheterization was performed. All sequences were acquired during breath holds of 10 to 15 s. Initially, a contiguous short-axis steady-state free precession cine stack (repetition time = 3.8 ms, echo time = 1.6 ms, 30 phases) was acquired, extending from the mitral valve annulus to the LV apex (8-mm slice thickness, no gap), to enable volumetric analysis of the left ventricle using the summation of disk method.

Late gadolinium enhancement (LGE) was evaluated 10 min after administration of a bolus of gadolinium–diethylene triamine penta-acetic acid (0.2 mmol/kg body weight, Magnevist, Schering, Germany) to identify regional myocardial fibrosis using a T_1-weighted inversion recovery gradient echo technique (repetition time = 7.1 ms, echo time = 3.1 ms; inversion time [TI] individually determined to null the myocardial signal; slice thickness, 8 mm; matrix, 256 × 192; number of acquisitions = 2). To enable accurate nullification of healthy myocardium, a TI optimization sequence was performed 8 min after gadolinium administration with a fast gradient echo, inversion recovery, and gated multiphase acquisition, commencing at an inversion time of 150 ms and increasing in 25 ms increments to 250 ms in a single mid-ventricular short-axis slice. LGE imaging was performed using standard long-axis views of the left ventricle and a contiguous short-axis stack from the mitral valve annulus to the LV apex. Regional fibrosis was identified by LGE within the myocardium, defined quantitatively by a myocardial post-contrast signal intensity 6 SD above that within a reference region of remote myocardium (without LGE) within the same slice (23). LGE was defined as being present only if it was identified in 2 orthogonal views.

To evaluate diffuse myocardial fibrosis, a histologically-validated post-contrast T_1 mapping sequence was used to cycle through acquisition of images obtained at the mid-LV short-axis level over a range of inversion times, as described previously (7). This electrocardiogram-triggered, inversion recovery–prepared, 2-dimensional fast gradient echo sequence used variable temporal sampling of k-space (VAST) (24) (Global Applied Science Laboratory, GE Healthcare). Ten images at the mid-LV short-axis level were acquired sequentially at increasing inversion times, pre-contrast (for non-contrast myocardial T_1 time; TI range, 75 to 1,875 ms) and also 15 min after administration of the bolus of gadolinium–diethylene triamine penta-acetic acid (TI range, 75 to 750 ms), and over a series of 3 to 5 breath holds. After image acquisition, the 10 short-axis images of varying TIs were transferred to an external computer for analysis using a dedicated research software package with a curve-fitting technique to generate T_1 maps (Cinetool, Global Applied Science Laboratory, GE Healthcare). For each short-axis image, a region of interest was drawn around the entire LV myocardium (excluding regions of LGE for post-contrast images) to calculate myocardial T_1 time. To account for the potential effect of glomerular filtration rate on gadolinium pharmacokinetics, correction values (25) were used to normalize post-contrast myocardial T_1 times to a matched state (eGFR = 90 ml/min/1.73 m^2). Non-contrast myocardial T_1 times were corrected for heart rate according to current recommendations (26). ECV, an alternative method of extracellular matrix expansion quantification, was derived using the previously described formula (27); $ECV = (1 - \text{hematocrit}) \times (\Delta R1_{myocardium}/\Delta R1_{blood})$, where $R1 = 1/T_1$ time.

Echocardiography protocol. Transthoracic echocardiography with a standard clinical protocol was performed on all patients immediately before cardiac catheterization. Diastolic function was assessed by a combination of mitral inflow pattern (E to A ratio) and early mitral annular velocities (e′, measured at the septal and lateral aspects of the mitral annulus in the apical 4-chamber view). Additionally, mitral E/e′ (septal, lateral, and mean) was chosen as an index of LV diastolic function. All measurements were made in accordance with the American Society of Echocardiography guidelines (28,29).

Data analysis. All echocardiographic and CMR images were interpreted by 2 experienced readers unaware of the subjects' clinical information and the results of other diagnostic tests. Endocardial and epicardial LV contours were drawn manually for each diastolic and systolic frame, excluding papillary muscles. An experienced operator without knowledge of patients' other test results analyzed the CC data.

Statistical analysis. All data are expressed as mean ± SD unless otherwise indicated. For all comparisons, a p value <0.05 was considered significant, and all reported p values are 2-tailed. Assuming a correlation coefficient between CMR measures of diffuse fibrosis (post-contrast T_1 time and ECV) and invasive measures of diastolic function (τ and β) of ≥ 0.55, a sample size of 20 was required to achieve a statistical power of 0.8, assuming a 2-tailed p value <0.05. Correlations of variables were determined by calculating the Pearson product moment. Multiple linear regression was used to determine the independence of correlations observed on simple linear regression. All analyses were conducted using Stata software version 11.1 (StataCorp., College Station, Texas).

Results

Clinical and demographic data. Twenty of 27 patients were included during the study period, and 7 patients were excluded (5 due to a retained pacing or defibrillator lead, 1 due to claustrophobia before CMR, and 1 due to severe renal impairment). Baseline characteristics of the study cohort are presented in Table 1. Most patients were male (80%), and the mean age was 49 ± 16 years. The median time elapsed since cardiac transplantation was 39 months (interquartile range: 13 to 61 months). Only 7 patients (35%) experienced exertional dyspnea.

Cardiac catheterization data. Invasive cardiac measurements obtained during right heart catheterization and coronary angiography are detailed in Table 2. β was derived from CC data for 17 patients (85%). In 1 patient, the aortic valve could not be crossed despite multiple attempts, and ventricular ectopy resulted in an uninterpretable PV dataset in 2 patients. Seventeen patients had no discernible coronary artery disease, 1 patient had an obstructive coronary artery lesion requiring subsequent percutaneous coronary intervention, and 2 patients had subtotally occluded coronary arteries that were managed without revascularization.

CMR and echocardiography data. CMR and transthoracic echocardiography were completed in all 20 patients,

Table 1 Baseline Characteristics

Age, yrs	49 ± 16
Males	16 (80)
Body mass index, kg/m^2	27.9 ± 4.6
Time since transplant, months	39 (13, 61)
Exertional dyspnea	
NYHA functional class	
I	13 (65)
II	7 (35)
III or IV	0 (0)
Medications	
Beta-blocker	3 (15)
Calcium-channel blocker	6 (30)
ACE inhibitor	8 (40)
ARB	4 (20)
Statin	18 (90)
Loop diuretic	4 (20)
Hematocrit	0.39 ± 0.04
eGFR, ml/min/1.73 m^2	66 ± 19

Values are mean ± SD, n (%), or and median (quartiles).
ACE = angiotensin-converting enzyme; ARB = angiotensin receptor blocker; eGFR = estimated glomerular filtration rate; NYHA = New York Heart Association.

and the results are displayed in Table 3. LGE was observed in 3 patients: 2 patients had subendocardially-based regional scar in the vascular distribution of a subtotally occluded coronary artery, and 1 patient had basal anteroseptal midwall LGE of unknown etiology. Post-contrast myocardial T_1 time was calculated in all 20 patients and, when corrected for eGFR, did not different significantly overall from uncorrected values (380 ± 82 ms vs. 375 ± 83 ms, p = 0.998). ECV could be determined in 16 patients (80%); in 4 patients, pre-contrast myocardial T_1 times could not be measured due to image artifact. ECV (26.8 ± 8.5%) and post-contrast T_1 time showed a strong negative correlation (r = −0.82, p = 0.0001) (Fig. 1).

Correlates of invasive measures of diastolic function. Linear regression modeling revealed no significant correlations between τ and patient baseline characteristics, catheterization, CMR, or echocardiography parameters. In particular, there was no correlation between τ and noncontrast myocardial T_1 time, post-contrast myocardial T_1 time, or ECV (p = NS for all comparisons).

Table 2 Cardiac Catheterization Data

Heart rate, beats/min	83 ± 14
Blood pressure, mm Hg	
Systolic	132 ± 24
Diastolic	79 ± 15
Cardiac index, l/min/m^2	3.2 ± 0.8
Right atrial pressure, mm Hg	3.6 ± 3.2
Pulmonary artery pressure, mm Hg	15.8 ± 4.2
Pulmonary capillary wedge pressure, mm Hg	7.5 ± 3.2
Left ventricular end-diastolic pressure, mm Hg	14.1 ± 8.2
Active ventricular relaxation constant (τ), ms	32.6 ± 7.4
Passive ventricular stiffness constant (β)	0.030 ± 0.016

Values are mean ± SD.

Table 3 Cardiac Magnetic Resonance Imaging and Echocardiography Data

Cardiac magnetic resonance imaging	
LVEDV indexed, ml/BSA	81 ± 20
LV stroke volume, ml	100 ± 38
LVEF, %	62 ± 8
LV mass indexed, g/BSA	56 ± 12
Presence of LGE	3 (15)
Noncontrast myocardial T_1 time, ms	937 ± 158
Noncontrast blood pool T_1 time, ms	1,435 ± 335
Post-contrast myocardial T_1 time, ms	380 ± 82
Post-contrast blood pool T_1 time, ms	229 ± 34
ECV, %	26.8 ± 8.5
Echocardiography	
Left atrial volume indexed, ml/m^2	59 ± 24
Mitral E velocity, cm/s	0.8 ± 0.2
Mitral A velocity, cm/s	0.4 ± 0.1
E/A ratio	1.9 ± 0.5
Deceleration time, ms	158 ± 31
Septal e′, cm/s	7.9 ± 1.7
Lateral e′, cm/s	12.4 ± 3.7
Mean e′, cm/s	10.1 ± 2.1
Septal E/e′ ratio	10.7 ± 2.4
Lateral E/e′ ratio	7.1 ± 2.0
Mean E/e′ ratio	8.9 ± 1.7

Values are mean ± SD or n (%).
BSA = body surface area; ECV = extracellular volume fraction; LGE = late gadolinium enhancement; LV = left ventricular; LVEDV = left ventricular end-diastolic volume; LVEF = left ventricular ejection fraction.

Univariate linear regression demonstrated significant correlations between β and both post-contrast myocardial T_1 time (r = −0.71, p = 0.001) (Fig. 2) and ECV (r = 0.58, p = 0.04) (Table 4). There were trends toward increased PCWP and LVEDP with increasing β (r = 0.47, p = 0.06, and r = 0.39, p = 0.12, respectively). No correlation was observed between β and noncontrast myocardial T_1

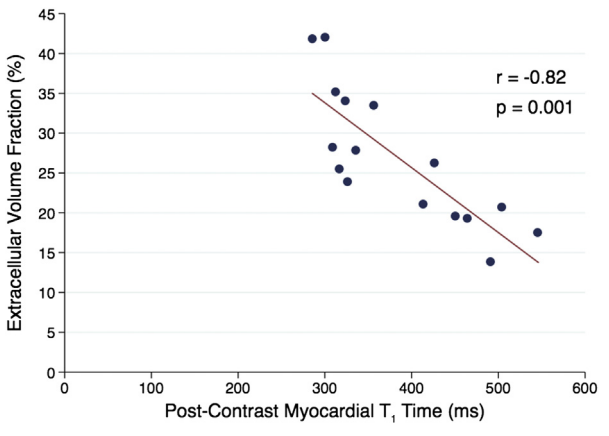

Figure 1 Post-Contrast Myocardial T_1 Time and Extracellular Volume Fraction

A significant negative correlation was observed between post-contrast T_1 time and extracellular volume fraction (r = −0.82, p = 0.001).

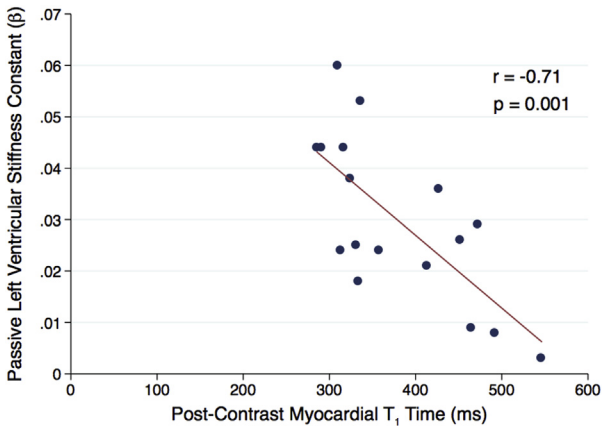

Figure 2 **Post-Contrast Myocardial T_1 Time and Passive Left Ventricular Stiffness Constant**

A significant positive negative correlation was observed between post-contrast myocardial T_1 time and passive left ventricular stiffness constant, β ($r = -0.71$, $p = 0.001$).

time or with CMR-derived LV volumetric parameters or echo-cardiographically-determined measures of LV diastolic function. Given the strong correlation between post-contrast myocardial T_1 time and ECV, these variables were entered into separate multiple linear regression analyses. After this analysis, only the correlation between β and post-contrast myocardial T_1 time remained significant.

Discussion

To our knowledge, this is the first study to demonstrate a physiological link between diffuse myocardial fibrosis assessed by post-contrast myocardial T_1 time, and an invasively-determined index of LV diastolic stiffness. Myocardial T_1 time, obtained at a single time point after contrast administration, and ECV, calculated from pre- and post-contrast myocardial and blood pool signals, both correlated with β, the load-independent LV passive stiffness constant.

Post-contrast myocardial T_1 times have previously been shown to correlate with the quantity of diffuse myocardial fibrosis observed in endomyocardial biopsy specimens (7,8), and several T_1 mapping studies have observed associations between reduced T_1 times and LV diastolic dysfunction as assessed by echocardiography (9–11). However, because echocardiographic studies use integrated backscatter and Doppler techniques that reflect both structural and functional changes in the myocardium, the precise mechanism of diastolic impairment has not been established. Compared with echocardiography, T_1 mapping by CMR is a tissue-specific modality that allows the unique opportunity to directly assess the structural components of the myocardium contributing to altered diastolic function. In the present

Table 4 **Predictors of Passive LV Stiffness Constant By Simple and Multiple Linear Regression**

	Simple Linear Regression		Multiple Linear Regression (Including Post-Contrast Myocardial T_1 Time)		Multiple Linear Regression (Including ECV)	
	r	p Value	β	p Value	β	p Value
Baseline characteristics						
Age	−0.21	0.4	0.11	0.7	−0.50	0.15
Body mass index	0.23	0.4	−0.15	0.5	0.18	0.5
NYHA functional class	0.07	0.8				
Time since transplantation	0.29	0.3	0.29	0.18	0.32	0.3
Cardiac catheterization parameters						
Heart rate	0.16	0.5	−0.08	0.8	0.24	0.4
Systolic blood pressure	−0.22	0.4	−0.28	0.4	0.37	0.5
Diastolic blood pressure	−0.10	0.7				
RAP	0.24	0.4				
PCWP	0.47	0.06	0.07	0.8	0.39	0.4
LVEDP	0.39	0.12	0.29	0.3	−0.04	0.9
Cardiac magnetic resonance imaging parameters						
LVEDV indexed	−0.25	0.3				
LVEF	−0.02	0.9				
LV mass indexed	−0.16	0.6	−0.12	0.6	−0.51	0.3
Noncontrast myocardial T_1 time	0.25	0.4				
Post-contrast myocardial T_1 time	−0.71	0.001	−0.80	0.02		
ECV	0.58	0.04			0.51	0.19
Echocardiography parameters						
Left atrial volume indexed	−0.21	0.4				
Mean E/e′ ratio	0.02	0.9				

LVEDP = left ventricular end-diastolic pressure; PCWP = pulmonary capillary wedge pressure; RAP = right atrial pressure; other abbreviations as in Tables 1 and 3.

study, by performing invasive PV measurements, active relaxation, an energy-dependent process, and passive filling could be evaluated independently and then correlated with T_1 time.

In patients with LV systolic dysfunction and heart failure with a normal ejection fraction, myocardial fibrosis is believed to contribute to increased passive LV stiffness (30). Given the diffuse nature of collagen deposition in cardiomyopathy, a noninvasive test for myocardial fibrosis is highly desirable, not just in terms of disease stratification, but also in the evaluation of newer therapies aimed at minimizing or reducing myocardial fibrosis in the treatment of heart failure. For example, therapies inhibiting the angiotensin II system may have antifibrotic properties (31,32), and T_1 mapping could theoretically be used to noninvasively monitor the amount of diffuse myocardial fibrosis present, allowing longitudinal assessment of the potential impact of such treatments on ventricular stiffness.

We observed correlations between post-contrast myocardial T_1 times and β, but not load-dependent measures of LV diastolic function such as LVEDP and the ratio of early mitral transmitral velocity to tissue Doppler mitral annular early diastolic velocity (E/e′, by echocardiography). In addition, active LV relaxation (τ) did not correlate with CMR indexes of diffuse myocardial fibrosis, suggesting that it is the intrinsic properties of the myocardium due to diffuse fibrosis and hence increased stiffness rather than perturbation of the energy-dependent active relaxation process that underlines the mechanism of diastolic dysfunction commonly observed in our patient cohort (33).

We found that although post-contrast myocardial T_1 time and ECV correlated with β, only the relationship between the post-contrast myocardial T_1 time and β remained statistically significant after multiple linear regression analyses. Noncontrast myocardial T_1 time exhibited no significant correlation with β. Post-contrast T_1 mapping times have been shown to correlate with the quantity of diffuse interstitial fibrosis seen on myocardial biopsy specimens (8), whereas noncontrast T_1 measurements, which are used to calculate ECV and native T_1 times, reflect a combination of both interstitial and myocardial signals. Therefore, precisely which altered tissue characteristics contribute to noncontrast values are uncertain. Various T_1 mapping approaches currently exist and are likely to provide different information about myocardial tissue characteristics. Nevertheless, our data identify a clear relationship between post-contrast myocardial T_1 time and LV passive stiffness. It is possible that other T_1 mapping protocols may demonstrate differing degrees of correlation with β, and future studies will be required to investigate this further.

Cardiac transplant recipients were chosen to form the study cohort because they provided opportunities to obtain invasive PV measurements at the time of clinically-indicated coronary angiography. Additionally, diffuse myocardial fibrosis has been shown to occur in ∼50% of cardiac transplant recipients (34), and the likelihood of pre-existing, and potentially confounding, cardiac conditions, such as hypertensive LV hypertrophy, significant valvular heart disease, and cardiomyopathy, was low. However, the generalizability of our findings to other cardiac disease states will need to be confirmed with further studies. For instance, in patients with ischemic cardiomyopathy, impairment of the energy-dependent process of active relaxation may also contribute to diastolic dysfunction without necessarily affecting T_1 time.

Study limitations. Because only a limited number of cardiac transplantations are performed, and a significant proportion of potentially eligible patients have contraindications to CMR, our overall study cohort size is small. Additionally, all recruited patients had either absent or mild symptoms of LV diastolic dysfunction, and overall intracardiac pressures were normal. Repeating our protocol in patients with more pronounced heart failure symptoms and higher intracardiac pressures would be of interest. The effect of various physiological maneuvers, such as exercise, on invasively-determined diastolic indexes was also not investigated in this study and may represent a focus for future research.

Conclusions

Diffuse myocardial fibrosis, assessed by post-contrast myocardial T_1 time, correlates with invasively-determined LV stiffness in cardiac transplant recipients. In patients with increased diffuse myocardial fibrosis, abnormal passive ventricular stiffness is therefore likely to be a major contributor to diastolic dysfunction. The ability to noninvasively evaluate ventricular stiffness using T_1 mapping in a variety of cardiomyopathies may enhance our understanding of the pathogenesis and natural history of these conditions and enable the therapeutic trials of putative antifibrotic agents.

Reprint requests and correspondence: Associate Professor Andrew J. Taylor, Alfred Hospital and Baker IDI Heart and Diabetes Research Institute, Heart Centre, Alfred Hospital, Commercial Road, Melbourne 3004, Victoria, Australia. E-mail: andrew.taylor@bakeridi.edu.au.

REFERENCES

1. Heling A, Zimmermann R, Kostin S, et al. Increased expression of cytoskeletal, linkage, and extracellular proteins in failing human myocardium. Circ Res 2000;86:846–53.
2. Sun Y, Weber KT. Cardiac remodelling by fibrous tissue: role of local factors and circulating hormones. Ann Med 1998;30 Suppl 1:3–8.
3. Maisch B. Ventricular remodeling. Cardiology 1996;87 Suppl 1:2–10.
4. Conrad CH, Brooks WW, Hayes JA, Sen S, Robinson KG, Bing OH. Myocardial fibrosis and stiffness with hypertrophy and heart failure in the spontaneously hypertensive rat. Circulation 1995;91:161–70.
5. Owan TE, Hodge DO, Herges RM, Jacobsen SJ, Roger VL, Redfield MM. Trends in prevalence and outcome of heart failure with preserved ejection fraction. N Engl J Med 2006;355:251–9.
6. Giannuzzi P, Temporelli PL, Bosimini E, et al. Independent and incremental prognostic value of Doppler-derived mitral deceleration time of early filling in both symptomatic and asymptomatic patients with left ventricular dysfunction. J Am Coll Cardiol 1996;28:383–90.

7. Iles L, Pfluger H, Phrommintikul A, et al. Evaluation of diffuse myocardial fibrosis in heart failure with cardiac magnetic resonance contrast-enhanced T1 mapping. J Am Coll Cardiol 2008;52:1574–80.
8. Sibley CT, Noureldin RA, Gai N, et al. T1 Mapping in cardiomyopathy at cardiac MR: comparison with endomyocardial biopsy. Radiology 2012;265:724–32.
9. Ng AC, Auger D, Delgado V, et al. Association between diffuse myocardial fibrosis by cardiac magnetic resonance contrast-enhanced T(1) mapping and subclinical myocardial dysfunction in diabetic patients: a pilot study. Circ Cardiovasc Imaging 2012;5:51–9.
10. Jellis C, Wright J, Kennedy D, et al. Association of imaging markers of myocardial fibrosis with metabolic and functional disturbances in early diabetic cardiomyopathy. Circ Cardiovasc Imaging 2011;4:693–702.
11. Ellims AH, Iles LM, Ling LH, Hare JL, Kaye DM, Taylor AJ. Diffuse myocardial fibrosis in hypertrophic cardiomyopathy can be identified by cardiovascular magnetic resonance, and is associated with left ventricular diastolic dysfunction. J Cardiovasc Magn Reson 2012;14:76.
12. Mongeon FP, Jerosch-Herold M, Coelho-Filho OR, Blankstein R, Falk RH, Kwong RY. Quantification of extracellular matrix expansion by CMR in infiltrative heart disease. J Am Coll Cardiol Img 2012;5:897–907.
13. Flett AS, Sado DM, Quarta G, et al. Diffuse myocardial fibrosis in severe aortic stenosis: an equilibrium contrast cardiovascular magnetic resonance study. Eur Heart J Cardiovasc Imaging 2012;13:819–26.
14. Puntmann VO, D'Cruz D, Smith Z, et al. Native myocardial t1 mapping by cardiovascular magnetic resonance imaging in subclinical cardiomyopathy in patients with systemic lupus erythematosus. Circ Cardiovasc Imaging 2013;6:295–301.
15. Nagueh SF, Middleton KJ, Kopelen HA, Zoghbi WA, Quinones MA. Doppler tissue imaging: a noninvasive technique for evaluation of left ventricular relaxation and estimation of filling pressures. J Am Coll Cardiol 1997;30:1527–33.
16. Ommen SR, Nishimura RA, Appleton CP, et al. Clinical utility of Doppler echocardiography and tissue Doppler imaging in the estimation of left ventricular filling pressures: a comparative simultaneous Doppler-catheterization study. Circulation 2000;102:1788–94.
17. Weiss JL, Frederiksen JW, Weisfeldt ML. Hemodynamic determinants of the time-course of fall in canine left ventricular pressure. J Clin Invest 1976;58:751–60.
18. Zile MR, Baicu CF, Gaasch WH. Diastolic heart failure–abnormalities in active relaxation and passive stiffness of the left ventricle. N Engl J Med 2004;350:1953–9.
19. Zile MR, Brutsaert DL. New concepts in diastolic dysfunction and diastolic heart failure: part II: causal mechanisms and treatment. Circulation 2002;105:1503–8.
20. Baan J, van der Velde ET, de Bruin HG, et al. Continuous measurement of left ventricular volume in animals and humans by conductance catheter. Circulation 1984;70:812–23.
21. Westermann D, Kasner M, Steendijk P, et al. Role of left ventricular stiffness in heart failure with normal ejection fraction. Circulation 2008;117:2051–60.
22. Zile MR, Brutsaert DL. New concepts in diastolic dysfunction and diastolic heart failure: Part I: diagnosis, prognosis, and measurements of diastolic function. Circulation 2002;105:1387–93.
23. Maron MS. Clinical utility of cardiovascular magnetic resonance in hypertrophic cardiomyopathy. J Cardiovasc Magn Reson 2012;14:13.
24. Saranathan M, Rochitte CE, Foo TK. Fast, three-dimensional free-breathing MR imaging of myocardial infarction: a feasibility study. Magn Reson Med 2004;51:1055–60.
25. Gai N, Turkbey EB, Nazarian S, et al. T1 mapping of the gadolinium-enhanced myocardium: adjustment for factors affecting interpatient comparison. Magn Reson Med 2011;65:1407–15.
26. Messroghli DR, Plein S, Higgins DM, et al. Human myocardium: single-breath-hold MR T1 mapping with high spatial resolution–reproducibility study. Radiology 2006;238:1004–12.
27. Flett AS, Hayward MP, Ashworth MT, et al. Equilibrium contrast cardiovascular magnetic resonance for the measurement of diffuse myocardial fibrosis: preliminary validation in humans. Circulation 2010;122:138–44.
28. Lang RM, Bierig M, Devereux RB, et al. Recommendations for chamber quantification: a report from the American Society of Echocardiography's Guidelines and Standards Committee and the Chamber Quantification Writing Group, developed in conjunction with the European Association of Echocardiography, a branch of the European Society of Cardiology. J Am Soc Echocardiogr 2005;18:1440–63.
29. Nagueh SF, Appleton CP, Gillebert TC, et al. Recommendations for the evaluation of left ventricular diastolic function by echocardiography. Eur J Echocardiogr 2009;10:165–93.
30. Maeder MT, Kaye DM. Heart failure with normal left ventricular ejection fraction. J Am Coll Cardiol 2009;53:905–18.
31. Brilla CG, Matsubara LS, Weber KT. Antifibrotic effects of spironolactone in preventing myocardial fibrosis in systemic arterial hypertension. Am J Cardiol 1993;71:12A–6A.
32. Brilla CG. Renin-angiotensin-aldosterone system and myocardial fibrosis. Cardiovasc Res 2000;47:1–3.
33. Tallaj JA, Kirklin JK, Brown RN, et al. Post-heart transplant diastolic dysfunction is a risk factor for mortality. J Am Coll Cardiol 2007;50:1064–9.
34. Winters GL, Costanzo-Nordin MR. Pathological findings in 2300 consecutive endomyocardial biopsies. Mod Pathol 1991;4:441–8.

Key Words: diastolic dysfunction ■ magnetic resonance imaging ■ myocardial fibrosis ■ T_1 mapping.